J Mater Sci (2007) 42:2208–2211
DOI 10.1007/s10853-006-1476-7

LETTER

Hardness variation across a $Zr_{57}Ti_5Cu_{20}Ni_8Al_{10}$ bulk metallic glass

Rong Chen · Fuqian Yang · Guojiang Fan · Peter K. Liaw

Received: 21 November 2006 / Accepted: 21 December 2006 / Published online: 6 February 2007
© Springer Science+Business Media, LLC 2007

Indentation test has recently been used to examine mechanical properties of bulk metallic glasses (BMGs). Donovan [1] observed the radial incipient cracks and the curving Hartmann lines in the deformation zone for the indentation of a $Pd_{40}Ni_{40}P_{20}$ BMG. Jana et al. [2] revealed several sets of slip-steps from shear bands for the Vickers indentation of $Pd_{42.1}Ni_{39.77}P_{18.13}$ and $Zr_{56.69}Cu_{26.96}Al_{10.95}Ni_{5.4}$ BMGs. Ramamurty et al. [3] used the bonded interface technique to examine the pattern of shear bands underneath the Vickers indentation in a $Pd_{42}Ni_{40}P_{18}$ BMG. Jana et al. [4] evaluated the subsurface deformation topology in the Vickers indentation of a $Zr_{57}Cu_{27}Al_{11}Ni_5$ BMG. Zhang et al. [5] investigated the evolution of shear bands in a Vitreloy 106 beneath a Vickers indentation. Yang et al. [6] observed surface wrinkling in the nanoindentation of a Zr-based BMG. Wang et al. [7] revealed the occurrence of serrated flow in the indentation of a Zr-based BMG. Golovin et al. [8] observed the occurrence of the pop-in in the loading phase for the indentation of a Pd-based BMG and noted that the dependence of the strain-serration on the indentation depth. Schuh and Nieh [9, 10] reported the serrated flow and suggested that the indentation-induced plastic flow could be a strong function of the indentation rate. Recently, Greer et al. [11] suggested that the absence of the serrated flow and the pop-in phenomenon at small indentation depth may be due to the lack of the resolution in instrument. However, there is little work on the dependence of the indentation deformation on the indentation position, related to the flow defect concentration from the solidification process in the preparation of bulk metallic glasses.

In this work, microindentation tests have been undertaken to study the nature of the indentation deformation of a $Zr_{57}Ti_5Cu_{20}Ni_8Al_{10}$ BMG. Especially, this work focuses on demonstrating the variation of the indentation behavior over the cross-section of the Zr-based BMG associated with the flow defect concentration from the solidification process. This allows us potentially to evaluate the inhomogeneity in bulk metallic glasses. The plastic energy dissipated in the indentation is also discussed.

A bulk metallic glass with the composition of $Zr_{57}Ti_5Cu_{20}Ni_8Al_{10}$ in atomic percent (at%) was used in the experiments. The cast rod of 5 mm in diameter and 60 mm in length was made at a cooling rate of 100 K/s, using a suction-casting method in an arc furnace via a pseudo-floating-melt state before casting to obtain a completely melted state [12]. A specimen of a disk shape with 5 mm in diameter and 1.5 mm in thickness was cut from the cast rod. The specimen was ground and polished before the indentation test to obtain two parallel surfaces of a mirror quality.

Microindentation tests were performed on a Micro-Combi Tester (CSM Instruments, Needham, MA), using a Vickers indenter on the circles of different radii with the same center as the specimen. The radii of the circles were 0.5, 1, 1.5 and 2.0 mm. The indentation load was 1,500 mN, and the loading and unloading rates were 50 mN/s without an intermediate pause. A pre-load of 5 mN was applied to the indenter before

R. Chen · F. Yang (✉)
Department of Chemical and Materials Engineering, University of Kentucky, Lexington, KY 40506, USA
e-mail: fyang0@engr.uky.edu

G. Fan · P. K. Liaw
Department of Materials Science and Engineering, University of Tennessee, Knoxville, TN 37994, USA

applying full indentation load to maintain the contact between the indenter and the surface of the specimen.

Figure 1 shows the indentation curves over the cross-section of the specimen at different positions. No serrated flow is observed from the loading curves under the test condition, which might be due to the limit of the resolution in the microindentation instrument. All of the unloading curves show the similarity at the upper portion of the unloading phase. The elastic recovery is independent of the indentation location. A light optical microscope is used to examine the indentation morphology; and no shear bands and pile-up are observed around all the indents over the specimen.

At the same indentation load, the maximum indentation depth decreases as the distance to the specimen center increases, i.e., less plastic deformation was introduced by the indentation close to the edge of the specimen. This demonstrates the inhomogeneous nature in the cast Zr-based BMG, which is likely due to the difference in the average amount of free volume per atom produced by the cooling process. At the cooling rate of 100 K/s, the material close to the outmost surface solidified first with gradual solidification toward to the center. A temperature gradient was created during the solidification process with the material near the outmost surface experiencing much faster cooling process. The temperature gradient causes heat transfer to the already solidified glass and induces structural recovery, resulting in the decrease in the average amount of free volume per atom. This leads to the increase in the resistance to the penetration of the indenter.

Figure 2 shows the variation of the indentation hardness of the specimen. The cast Zr-based BMG has higher hardness away from the center of the specimen.

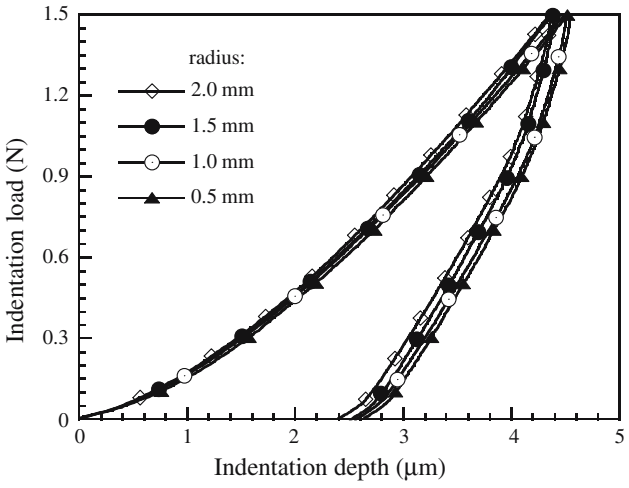

Fig. 1 Indentation curves of the $Zr_{57}Ti_5Cu_{20}Ni_8Al_{10}$ BMG for the indentations at different positions over the specimen surface

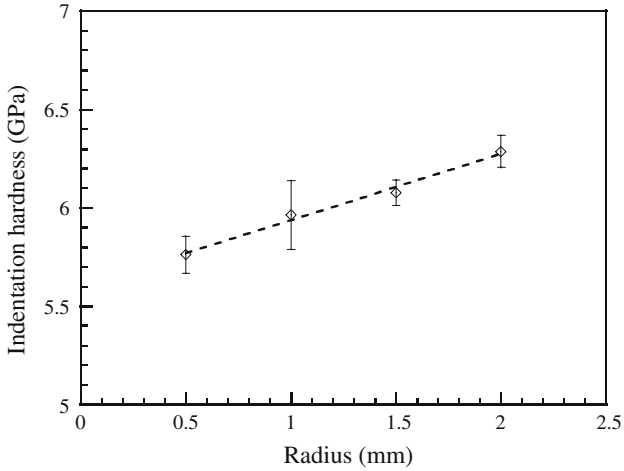

Fig. 2 Dependence of the indentation hardness on the indentation location

The results suggest that there was a gradient of the flow defect concentration over the Zr-based BMG rod, which was created by the non-uniform solidification process at the cooling rate of 100 K/s. This gradient created inhomogeneous nature, and introduced the variation of local mechanical response to external loading, as shown by the indentation test.

According to Cohen and Turnbull [13], the flow defect concentration, c_f, in a bulk metallic glass can be expressed as

$$c_f = e^{-\alpha\Omega_\square/\langle\Omega_f\rangle} \quad (1)$$

where α is a geometrical factor in the order of unity, $\Omega_\square$ is the critical amount of free volume to form a defect, and $\langle\Omega_f\rangle$ is the average amount of free volume per atom. The parameter of $\langle\Omega_f\rangle/\alpha\Omega_\square$ represents the reduced average free volume per atom. The fluidity of a BMG is related to the flow defect concentration as [13]

$$\mu = \upsilon c_f = \upsilon e^{-\alpha\Omega_\square/\langle\Omega_f\rangle} \quad (2)$$

where μ is the fluidity of the BMG and υ is a constant depending on the molecular size and the mobility of molecules. The structural recovery due to the temperature gradient lowers the average amount of free volume in the material near the outmost surface with maxima at the center and minimum near the outmost surface. The fluidity of the Zr-based BMG decreases with the increase in the distance away from the center. Thus the highest indentation hardness is expected for the indentation near the outmost surface, which is supported by the experimental results.

To examine the dependence of the indentation hardness on the indentation load, indentation tests

were performed along a circle of 1.5 mm in radius over the specimen surface in the load range of 200–5,000 mN. Figure 3 shows the effect of the indentation load on the indentation hardness. The indentation hardness decreases with the increase in the indentation load. This might be due to the formation and propagation of shear bands underneath the indentation, which induces strain softening as observed by Bhowmick et al. [14] and Bei et al. [15].

The plastic energy, E_{plastic}, dissipated during a loading–unloading cycle can be calculated from the area of the indentation curve as [16, 17]

$$E_{\text{plastic}} = \int_0^{\delta_{\max}} Fd\delta - \int_{\delta_r}^{\delta_{\max}} Fd\delta \tag{3}$$

where $\delta_{\max}$ is the maximum indentation depth at the maximum indentation load of $F_{\max}$ and δ_r is the residual indentation depth after totally removing the load. Figure 4 shows the variation of the plastic energy dissipated in the indentation over the specimen. The plastic energy dissipated in the indentation decreases as the distance to the specimen center increases. This is due to the decrease of the flow defect concentration with the distance, which imposes higher resistance to the penetration of the indenter. At the same indentation load, shallow indentation was produced and less energy was dissipated.

Using the indentation technique, the variation of the indentation deformation in the $Zr_{57}Ti_5Cu_{20}Ni_8Al_{10}$ BMG was studied over the specimen surface. The indentation tests were performed over a series of circles with the center of the circles the same as that of the specimen. It was found that the indentation hardness increases with the increase in the distance to the specimen center. This demonstrated the inhomogeneous nature in the cast Zr-BMG rod, and there was a gradient in the flow defect concentration associated with the rapid solidification process. The plastic energy dissipated in the indentation decreased with the increase in the distance to the center likely due to lower flow defect concentration. The results show the potential to evaluate the inhomogeneity in bulk metallic glasses using the indentation technique.

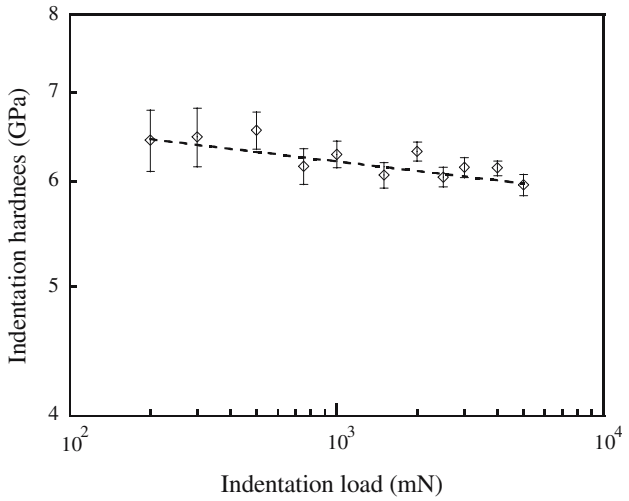

Fig. 3 Dependence of the indentation hardness on the indentation load

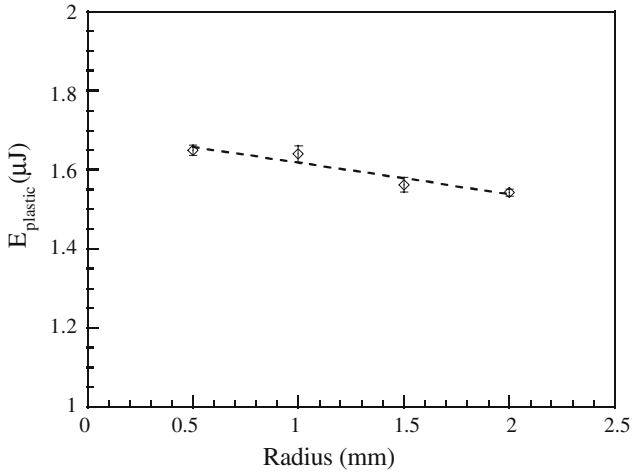

Fig. 4 Dependence of the plastic energy on the indentation position

Acknowledgement FY is grateful for support from the NSF Grant CMS-0508989 and the support from General Motors Corporation. PKL and GF are supported by the International Materials Institutes (IMI) program, DMR-0231320, with Dr. C. Huber as the program director.

References

1. Donovan PE (1989) J Mater Sci 24:523
2. Jana S, Ramamurty U, Chattopadhyay K, Kawamura Y (2004) Mater Sci Eng A 375–377:1191
3. Ramamurty U, Jana S, Kawamura Y, Chattopadhyay K (2005) Acta Mater 53:70
4. Jana S, Bhowmick R, Kawamura Y, Chattopadhyay K, Ramamurty U (2004) Intermetallics 12:1097
5. Zhang H, Jing X, Subhash G, Kecskes LJ, Dowding RJ (2005) Acta Mater 53:3849
6. Yang FQ, Geng K, Liaw PK, Fan GJ, Choo H (2007) Acta Mater 55:321
7. Wang JG, Choi BW, Nieh TG, Liu CT (2000) J Mater Res 15:798
8. Golovin YI, Ivogin VI, Khonik VA, Kitagawa K, Tyurin AI (2001) Scrip Mater 45:947
9. Schuh CA, Nieh TG (2004) J Mater Res 19:47
10. Schuh CA, Nieh TG (2003) Acta Mater 51:87
11. Greer AL, Castellero A, Madge SV, Walker IT, Wilde JR (2004) Mater Sci Eng A 375–377:1182

12. Wang GY, Liaw PK, Peter WH, Yang B, Yokoyama Y, Benson ML, Green BA, Kirkham MJ, Ahite SA, Saleh TA, McDaniels RL, Steward RV, Buchanan RA, Liu CT, Brooks CR (2004) Intermetallics 12:885
13. Cohen MH, Turnbull D (1959) J Chem Phys 31:1164
14. Bhowmick R, Raghavan R, Chattopadhyay K, Ramamurty U (2006) Acta Mater 54:4221
15. Bei H, Xie S, George EP (2006) Phys Rev Lett 96: Art. No. 105503
16. Yang FQ, Peng LL, Okazaki K (2004) Metall Mater Trans A 35:3323
17. Yang FQ, Du WW, Okazaki K (2005) J Mater Res 20:1172